

1 Hysteresis

The special feature of ferromagnetic and ferrimagnetic materials is that spontaneous magnetization sets in below a material-specific temperature (Curie point). The elementary atomic magnets are then aligned in parallel within macroscopic regions. These so-called Weiss' domains are normally oriented so that no magnetic effect is perceptible. But it is different when a ferromagnetic body is placed in a magnetic field and the flux density B as a function of the magnetic field strength H is measured with the aid of a test coil. Proceeding from $H = 0$ and $B = 0$, the so-called initial magnetization curve is first obtained. At low levels of field strength, those domains that are favorably oriented to the magnetic field grow at the expense of those that are not. This produces what are called wall displacements. At higher field strength, whole domains overturn magnetically – this is the steepest part of the curve – and finally the magnetic moments are moved out of the preferred states given by the crystal lattice into the direction of the field until saturation is obtained, i.e. until all elementary magnets in the material are in the direction of the field. If H is now reduced again, the B curve is completely different. The relationship shown in the hysteresis loop (Fig. 1) is obtained.

1.1 Hysteresis loop

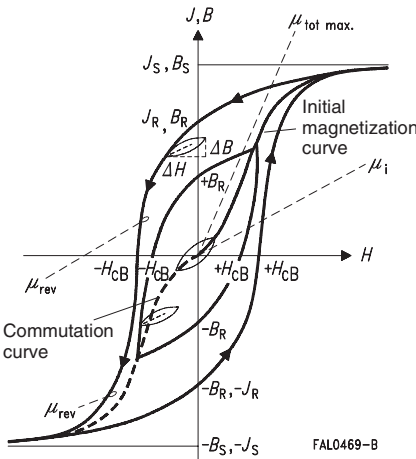


Fig. 1
Magnetization curve
(schematic)

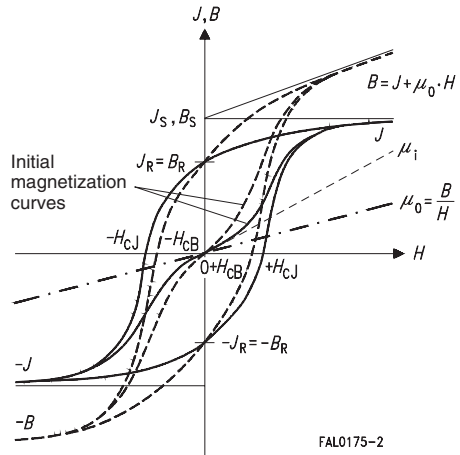


Fig. 2
Hysteresis loops for different
excitations and materials

Magnetic field strength $H = \frac{I \cdot N}{l} = \frac{\text{ampere-turns}}{\text{length in m}} \quad \left[\frac{A}{m} \right]$

Magnetic flux density $B = \frac{\Phi}{A} = \frac{\text{magnetic flux}}{\text{permeated area}} \quad \left[\frac{Vs}{m^2} \right] = [T (\text{Tesla})]$

General
Definitions

$$\text{Polarization } J \qquad J = B - \mu_0 H \qquad \mu_0 \cdot H \ll J \Rightarrow B \approx J$$

General relationship between B and H :

$$B = \mu_0 \cdot \mu_r(H) \cdot H \qquad \mu_0 = \text{magnetic field constant}$$

$$\mu_0 = 1,257 \cdot 10^{-6} \left[\frac{\text{Vs}}{\text{Am}} \right]$$

$$\mu_r = \text{relative permeability}$$

In a vacuum, $\mu_r = 1$; in ferromagnetic or ferrimagnetic materials the relation $B(H)$ becomes nonlinear and the slope of the hysteresis loop $\mu_r \gg 1$.

1.2 Basic parameters of the hysteresis loop

1.2.1 Initial magnetization curve

The initial magnetization curve describes the relationship $B = \mu_r \mu_0 H$ for the first magnetization following a complete demagnetization. By joining the end points of all “sub-loops”, from $H = 0$ to $H = H_{\max}$, (as shown in Figure 1), we obtain the so-called commutation curve (also termed normal or mean magnetization curve), which, for magnetically soft ferrite materials, coincides with the initial magnetization curve.

1.2.2 Saturation magnetization B_S

The saturation magnetization B_S is defined as the maximum flux density attainable in a material (i.e. for a very high field strength) at a given temperature; above this value B_S , it is not possible to further increase $B(H)$ by further increasing H .

Technically, B_S is defined as the flux density at a field strength of $H = 1200 \text{ A/m}$. As is confirmed in the actual magnetization curves in the chapter on “Materials”, the $B(H)$ characteristic above 1200 A/m remains roughly constant (applies to all ferrites with high initial permeability, i.e. where $\mu \geq 100$).

1.2.3 Remanent flux density $B_R(H)$

The remanent flux density (residual magnetization density) is a measure of the degree of residual magnetization in the ferrite after traversing a hysteresis loop. If the magnetic field H is subsequently reduced to zero, the ferrite still has a material-specific flux density $B_R \neq 0$ (see Fig. 1: intersection with the ordinate $H = 0$).

1.2.4 Coercive field strength H_C

The flux density B can be reduced to zero again by applying a specific opposing field $-H_C$ (see Fig. 1: intersection with the abscissa $B = 0$).

The demagnetized state can be restored at any time by:

- traversing the hysteresis loop at a high frequency and simultaneously reducing the field strength H to $H = 0$.
- by exceeding the Curie temperature T_C .

2 Permeability

Different relative permeabilities μ are defined on the basis of the hysteresis loop for the various electromagnetic applications.

2.1 Initial permeability μ_i

$$\mu_i = \frac{1}{\mu_0} \cdot \frac{\Delta B}{\Delta H} \quad (\Delta H \rightarrow 0)$$

The initial permeability μ_i defines the relative permeability at very low excitation levels and constitutes the most important means of comparison for soft magnetic materials. According to IEC 60401, μ_i is defined using closed magnetic circuits (e.g. a closed ring-shaped cylindrical coil) for $f \leq 10$ kHz, $B < 0,25$ mT, $T = 25$ °C.

2.2 Effective permeability μ_e

Most core shapes in use today do not have closed magnetic paths (Only ring, double E or double-aperture cores have closed magnetic circuits.), rather the circuit consists of regions where $\mu_i \neq 1$ (ferrite material) and $\mu_i = 1$ (air gap). Fig. 3 shows the shape of the hysteresis loop of a circuit of this type.

In practice, an effective permeability μ_e is defined for cores with air gaps.

$$\mu_e = \frac{1}{\mu_0 N^2} \sum \frac{l}{A}$$

$$\sum \frac{l}{A} = \text{form factor}$$

L = inductance
N = number of turns

It should be noted, for example, that the loss factor $\tan \delta$ and the temperature coefficient for gapped cores reduce in the ratio μ_e/μ_i compared to ungapped cores.

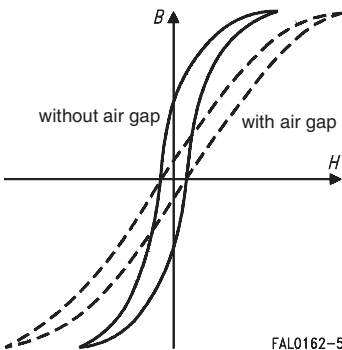


Fig. 3
Comparison of hysteresis loops for a core with and without an air gap

The following approximation applies for an air gap $s \ll l_e$:

$$\mu_e = \frac{\mu_i}{1 + \frac{s}{l_e} \cdot \mu_i}$$

s = width of air gap

l_e = effective magnetic path length

For more precise calculation methods, see for example E.C. Snelling, "Soft ferrites", 2nd edition.

2.3 Apparent permeability μ_{app}

$$\mu_{app} = \frac{L}{L_0} = \frac{\text{inductance with core}}{\text{inductance without core}}$$

The definition of μ_{app} is particularly important for specification of the permeability for coils with tubular, cylindrical and threaded cores, since an unambiguous relationship between initial permeability μ_i and effective permeability μ_e is not possible on account of the high leakage inductances. The design of the winding and the spatial correlation between coil and core have a considerable influence on μ_{app} . A precise specification of μ_{app} requires a precise specification of the measuring coil arrangement.

2.4 Complex permeability $\bar{\mu}$

To enable a better comparison of ferrite materials and their frequency characteristics at very low field strengths (in order to take into consideration the phase displacement between voltage and current), it is useful to introduce μ as a complex operator, i.e. a complex permeability $\bar{\mu}$, according to the following relationship:

$$\bar{\mu} = \mu_s' - j \cdot \mu_s''$$

where, in terms of a series equivalent circuit, (see Fig. 5)

μ_s' is the relative real (inductance) component of $\bar{\mu}$

and μ_s'' is the relative imaginary (loss) component of $\bar{\mu}$.

Using the complex permeability $\bar{\mu}$, the (complex) impedance of the coil can be calculated:

$$\bar{Z} = j \omega \bar{\mu} L_0$$

where L_0 represents the inductance of a core of permeability $\mu_r = 1$, but with unchanged flux distribution.

(cf. also section 4.1: information on $\tan \delta$)

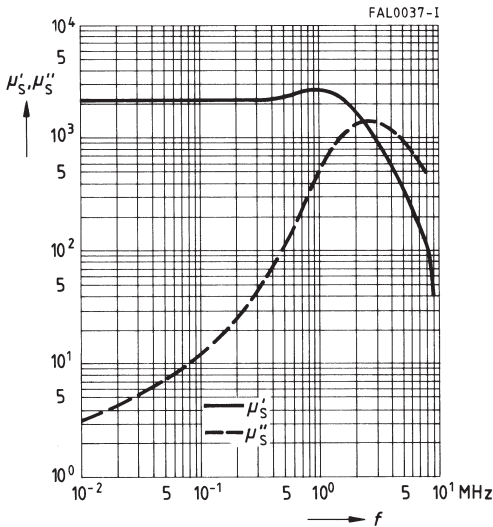


Fig. 4

Complex permeability versus frequency

(measured on R10 toroids, N 48 material, measuring flux density $\hat{B} \leq 0,25$ mT)

Fig. 4 shows the characteristic shape of the curves of μ'_S and μ''_S as functions of the frequency, using N 48 material as an example. The real component μ'_S is constant at low frequencies, attains a maximum at higher frequencies and then drops in approximately inverse proportion to f . At the same time, μ''_S rises steeply from a very small value at low frequencies to attain a distinct maximum and, past this, also drops as the frequency is further increased.

The region in which μ'_S decreases sharply and where the μ''_S maximum occurs is termed the cut-off frequency f_{cutoff} . This is inversely proportional to the initial permeability of the material (Snoek's law).

2.5 Reversible permeability μ_{rev}

$$\mu_{\text{rev}} = \frac{1}{\mu_0} \cdot \lim_{\Delta H \rightarrow 0} \left(\frac{\Delta B}{\Delta H} \right)_{H_-} \quad (\text{Permeability with superimposed DC field } H_-)$$

In order to measure the reversible permeability μ_{rev} , a small measuring alternating field is superimposed on a DC field. In this case μ_{rev} is heavily dependent on H_- , the core geometry and the temperature.

Important application areas for DC field-superimposed, i.e. magnetically biased coils are broadband transformer systems (feeding currents with signal superposition) and power engineering (shifting the operating point) and the area known as "nonlinear chokes" (cf. chapter on RM cores). For the magnetic bias curves as a function of the excitation H_- see the chapter on "SIFERRIT materials".

2.6 Amplitude permeability μ_a , A_{L1} value

$$\mu_a = \frac{\hat{B}}{\mu_0 \hat{H}} \quad (\text{Permeability at high excitation})$$

\hat{B} = peak value of flux density
 \hat{H} = peak value of field strength

For frequencies well below cut-off frequency, μ_a is not frequency-dependent but there is a strong dependence on temperature. The amplitude permeability is an important definition quantity for power ferrites. It is defined for specific core types by means of an A_{L1} value for $f \leq 10$ kHz, $B = 320$ mT (or 200 mT), $T = 100$ °C.

$$A_{L1} = \frac{\mu_0 \cdot \mu_a}{\sum \frac{l}{A}}$$

3 Magnetic core shape characteristics

Permeabilities and also other magnetic parameters are generally defined as material-specific quantities. For a particular core shape, however, the magnetic data are influenced to a significant extent by the geometry. Thus, the inductance of a slim-line ring core coil is defined as:

$$L = \mu_r \cdot \mu_0 \cdot N^2 \cdot \frac{A}{l}$$

Due to their geometry, soft magnetic ferrite cores in the field of such a coil change the flux parameters in such a way that it is necessary to specify a series of effective core shape parameters in each data sheet. The following are defined:

l_e effective magnetic length
 A_e effective magnetic cross section
 A_{\min} min. magnetic cross section of the core
 (required to calculate the max. flux density)
 $V_e = A_e \cdot l_e$ effective magnetic volume

With the aid of these parameters, the calculation for ferrite cores with complicated shapes can be reduced to the considerably more simple problem of an imaginary ring core with the same magnetic properties. The basis for this is provided by the methods of calculation according to IEC 60205, IEC 60205A and IEC 60205B, which allow the following factors $\Sigma l/A$ and A_L to be calculated:

3.1 Form factor

$$\sum \frac{l}{A} = \frac{l_e}{A_e}$$

The inductance L can then be calculated as follows:

$$L = \frac{\mu_e \cdot \mu_0 \cdot N^2}{\sum \frac{l}{A}}$$

where μ_e denotes the effective permeability or another permeability μ_{rev} or μ_a (or μ_i for cores with a closed magnetic path) adapted for the B/H range in question.

3.2 Inductance factor, A_L value

$$A_L = \frac{L}{N^2} = \frac{\mu_e \cdot \mu_0}{\sum \frac{l}{A}}$$

A_L is the inductance referred to number of turns = 1. Therefore, for a defined number of turns N :

$$L = A_L \cdot N^2$$

3.3 Tolerance code letters

The tolerances of the A_L are coded by the letters in the third block of the ordering code in conformity with IEC 60062.

Code letter	Tolerance of A_L value	Code letter	Tolerance of A_L value
A	± 3 %	K	± 10 %
B	± 4 %	L	± 15 %
C	± 6 %	M	± 20 %
D	± 8 %	Q	+ 30 / - 10 %
E	± 7 %	R	+ 30 / - 20 %
G	± 2 %	U	+ 80 / - 0 %
H	± 12 %	X	filling letter
J	± 5 %	Y	+ 40 / - 30 %

The tolerance values available are given in the individual data sheets.

4 Definition quantities in the small-signal range

4.1 Loss factor $\tan \delta$

Losses in the small-signal range are specified by the loss factor $\tan \delta$.

Based on the impedance \bar{Z} (cf. also section 2.4), the loss factor of the core in conjunction with the complex permeability $\bar{\mu}$ is defined as

$$\tan \delta_s = \frac{\mu_s''}{\mu_s'} = \frac{R_s}{\omega L_s} \quad \text{and} \quad \tan \delta_p = \frac{\mu_p''}{\mu_p'} = \frac{\omega \cdot L_p}{R_p}$$

where R_s and R_p denote the series and parallel resistance and L_s and L_p the series and parallel inductance respectively.

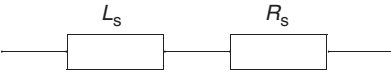


Fig. 5
Lossless series inductance L_s with loss resistance R_s resulting from the core losses.

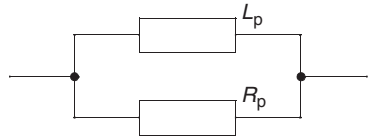


Fig. 6
Lossless parallel inductance L_p with loss resistance R_p resulting from the core losses.

From the relationships between series and parallel circuits we obtain:

$$\mu'_p = \mu'_s \cdot (1 + (\tan \delta)^2)$$

$$\mu''_p = \mu''_s \cdot \left(1 + \left(\frac{1}{\tan \delta}\right)^2\right)$$

4.2 Relative loss factor $\tan \delta / \mu_i$

In gapped cores the material loss factor $\tan \delta$ is reduced by the factor μ_e / μ_i . This results in the relative loss factor $\tan \delta_e$ (cf. also section 2.2):

$$\tan \delta_e = \frac{\tan \delta}{\mu_i} \cdot \mu_e$$

The table of material properties lists the relative loss factor $\tan \delta / \mu_i$. This is determined in accordance with IEC 60401 at $f = 10$ kHz, $B = 0,25$ mT, $T = 25$ °C.

4.3 Quality factor Q

The ratio of reactance to total resistance of an induction coil is known as the quality factor Q .

$$Q = \frac{\omega L}{R_L} = \frac{\text{reactance}}{\text{total resistance}}$$

The total quality factor Q is the reciprocal of the total loss factor $\tan \delta$ of the coil; it is dependent on the frequency, inductance, temperature, winding wire and permeability of the core.

4.4 Hysteresis loss resistance R_h and hysteresis material constant η_B

In transformers, in particular, the user cannot always be content with very low saturation. The user requires details of the losses which occur at higher saturation, e.g. where the hysteresis loop begins to open.

Since this hysteresis loss resistance R_h can rise sharply in different flux density ranges and at different frequencies, it is measured in accordance with IEC 60401 for μ_i values greater than 500 at $B_1 = 1,5$ and $B_2 = 3$ mT ($\Delta B = 1,5$ mT), a frequency of 10 kHz and a temperature of 25 °C (for $\mu_i < 500$: $f = 100$ kHz). The hysteresis loss factor $\tan \delta_h$ can then be calculated from this.

$$\tan \delta_h = \frac{R_h}{\omega \cdot L} = \tan \delta(B_2) - \tan \delta(B_1)$$

For the hysteresis material constant η_B we obtain:

$$\eta_B = \frac{\tan \delta_h}{\mu_e \cdot \Delta \hat{B}}$$

The hysteresis material constant, η_B , characterizes the material-specific hysteresis losses and is a quantity independent of the air gap in a magnetic circuit.

The hysteresis loss factor of an inductor can be reduced, at a constant flux density, by means of an (additional) air gap

$$\tan \delta_h = \eta_B \cdot \Delta \hat{B} \cdot \mu_e$$

For further details on the measurement techniques see IEC 60367-1.

5 Definition quantities in the high-excitation range

While in the small-signal range ($H \leq H_c$), i.e. in filter and broadband applications, the hysteresis loop is generally traversed only in lancet form (Fig. 2), for power applications the hysteresis loop is driven partly into saturation. The defining quantities are then

μ_{rev} reversible permeability in the case of superimposition with a DC signal
(operating point for power transformers)

μ_a amplitude permeability and

P_V core losses.

5.1 Core losses P_V

The losses of a ferrite core or core set P_V is proportional to the area of the hysteresis loop in question. It can be divided into three components:

$$P_V = P_{V, \text{hysteresis}} + P_{V, \text{eddycurrent}} + P_{V, \text{residual}}$$

Owing to the high specific resistance of ferrite materials, the eddy current losses in the frequency range common today (1 kHz - 2 MHz) may be practically disregarded except in the case of core shapes having a large cross-sectional area.

The power loss P_V is a function of the temperature T , the frequency f , the flux density B and is of course dependent on ferrite material and core shape.

The temperature dependence can generally be approximated by means of a third-order polynomial, while

$$P_V(f) \sim f^{(1+x)} \quad 0 \leq x \leq 1$$

applies for the frequency dependence and

$$P_V(B) \sim B^{(2+y)} \quad 0 \leq y \leq 1$$

for the flux density dependence. The coefficients x and y are dependent on core shape and material, and there is a mutual dependence between the coefficients of the definition quantity (e.g. T) and the relevant parameter set (e.g. f, B).

In the case of cores which are suitable for power applications, the total core losses P_V are given explicitly for a specific frequency f , flux density B and temperature T in the relevant data sheets.

When determining the total power loss for an inductive component, the winding losses must also be taken into consideration in addition to the core-specific losses.

$$P_{V \text{ tot}} = P_{V \text{ core}} + P_{V \text{ winding}}$$

where, in addition to insulation conditions in the given frequency range, skin effect and proximity effect must also be taken into consideration for the winding.

5.2 Performance factor ($PF = f \cdot B_{\text{max}}$)

The performance factor is a measure of the maximum power which a ferrite can transmit, whereby it is generally assumed that the loss does not exceed 300 kW/m³. Heat dissipation values of this order are usually assumed when designing small and medium-sized transformers. Increasing the performance factor will either enable an increase of the power that can be transformed by a core of identical design, or a reduction in component size if the transformed power is not increased.

If the performance factors of different power transformer materials are plotted as a function of frequency, only slight differences are observed at low frequencies (< 300 kHz), but these differences become more pronounced with increasing frequency. This diagram can be used to determine the optimum material for a given frequency range (for diagram see page 46).

6 Influence of temperature

6.1 $\mu(T)$ curve, Curie temperature T_C

The initial permeability μ_i as a function of T is given for all materials (see chapter on SIFERRIT materials). Important parameters for a $\mu(T)$ curve are the position of the secondary permeability maximum (SPM) and the Curie temperature. Minimum losses occur at the SPM temperature.

Above the Curie temperature T_C ferrite materials lose their ferrimagnetic properties, i.e. μ_i drops to $\mu_i = 1$. This means that the parallel alignment of the elementary magnets (spontaneous magnetization) is destroyed by increasing thermal activation. This phenomenon is reversible, i.e. when the temperature is reduced below T_C again, the ferrimagnetic properties are restored.

6.2 Temperature coefficient of permeability α

By definition the temperature coefficient α represents a straight line of average gradient between the reference temperatures T_1 and T_2 . If the $\mu(T)$ curve is approximately linear in this temperature range, this is a good approximation; in the case of heavily pronounced maxima, as occur particularly with highly permeable broadband ferrites, however, this is less true. The following applies:

$$\alpha = \frac{\mu_{i2} - \mu_{i1}}{\mu_{i1}} \cdot \frac{1}{T_2 - T_1}$$

μ_{i1} = initial permeability μ_i at $T_1 = 25^\circ\text{C}$

μ_{i2} = the initial permeability μ_i associated with the temperature T_2

6.3 Relative temperature coefficient α_F

$$\alpha_F = \frac{\alpha}{\mu_i} = \frac{\mu_{i2} - \mu_{i1}}{\mu_{i2} \cdot \mu_{i1}} \cdot \frac{1}{T_2 - T_1}$$

In a magnetic circuit with an air gap and the effective permeability μ_e the temperature coefficient is reduced by the factor μ_e/μ_i (cf. also section 2.4).

6.4 Permeability factor

The first factor in the equation for determining the relative temperature coefficient $\frac{\mu_{i2} - \mu_{i1}}{\mu_{i2} \cdot \mu_{i1}}$ is known as the permeability factor.

In the case of SIFERRIT materials for resonant circuits, the temperature dependence of the permeability factor can be seen from the relevant diagram.

6.5 Effective temperature coefficient α_e

$$\alpha_e = \frac{\mu_e}{\mu_i} \cdot \alpha$$

In the case of the ferrite materials for filter applications, the α/μ_i values for the ranges $25 \dots 55^\circ\text{C}$ and $5 \dots 25^\circ\text{C}$ are given in the table of material properties.

The effective permeability μ_e is required in order to calculate α_e ; therefore this is given for each core in the individual data sheets.

6.6 Relationship between the change in inductance and the permeability factor

The relative change in inductance between two temperature points can be calculated as follows:

$$\frac{L_2 - L_1}{L_1} = \frac{\alpha}{\mu_i} \cdot (T_2 - T_1) \cdot \mu_e$$

$$\frac{L_2 - L_1}{L_1} = \frac{\mu_{i2} - \mu_{i1}}{\mu_{i2} \cdot \mu_{i1}} \mu_e$$

6.7 Temperature dependence of saturation magnetization

The saturation magnetization B_S drops monotonically with temperature and at T_C has fallen to $B_S = 0$ mT. The drop for $B_S(25^\circ\text{C})$ and $B_S(100^\circ\text{C})$, i.e. the main area of application for the ferrites, can be taken from the table of material properties.

6.8 Temperature dependence of saturation-dependent permeability (amplitude permeability)

It can be seen from the $\mu_a(B)$ curves for the different materials that μ_a exhibits a more pronounced maximum with increasing temperature and drops off sooner on account of decreasing saturation.

7 Disaccommodation

Ferrimagnetic states of equilibrium can be influenced by mechanical, thermal or magnetic changes (shocks). Generally, an increase in permeability occurs when a greater mobility of individual magnetic domains is attained through the external application of energy. This state is not temporally stable and returns logarithmically with time to the original state.

7.1 Disaccommodation coefficient d

$$d = \frac{\mu_{i1} - \mu_{i2}}{\mu_{i1} \cdot (\lg t_2 - \lg t_1)}$$

where μ_{i1} = permeability at time t_1
 μ_{i2} = permeability at time t_2 and $t_2 > t_1$

7.2 Disaccommodation factor DF

$$DF = \frac{d}{\mu_{i1}}$$

Accordingly, a change in inductance can be calculated with the aid of DF :

$$\frac{L_1 - L_2}{L_1} = DF \cdot \mu_e \cdot \log \frac{t_2}{t_1}$$

8 General mechanical, thermal, electrical and magnetic properties of ferrites

Typical figures for the mechanical and thermal properties of ferrites

Tensile strength	approx. 30 MPa/mm ²
Compressive strength	approx. 800 MPa/mm ²
Vickers hardness HV ₁₅	approx. 600 MPa/mm ²
Modulus of elasticity	approx. 150000 N/mm ²
Fracture toughness K _{1c}	approx. 0,8 ... 1,1 MPa·m ^{1/2}
Thermal conductivity	approx. 4 ... 7·10 ⁻³ J/mm·s·K
Coefficient of linear expansion	approx. 7 ... 10 ·10 ⁻⁶ 1/K
Specific heat	approx. 0,7 J/g·K

8.1 Mechanical properties

Ferrite cores have to meet mechanical requirements during assembling and for a growing number of applications. Since ferrites are ceramic materials one has to be aware of the special behavior under mechanical load.

As valid for any ceramic material, ferrite cores are brittle and sensitive to any shock, fast changing or tensile load. Especially high cooling rates under ultrasonic cleaning and high static or cyclic loads can cause cracks or failure of the ferrite cores.

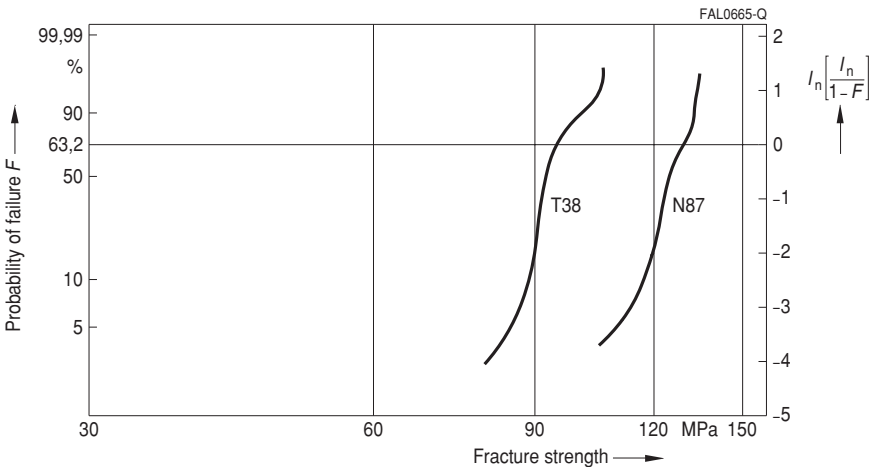


Fig. 7 Weibull plot of fracture strength values of the materials T38 and N87

There are two modes of crack growth: fast (critical) or slow (subcritical) crack propagation. In the first case spontaneous breakdown occurs. In the second case the crack propagates slowly during static or cycling loading, and then the sample can only fail if a critical crack length is achieved. According to the linear elastic fracture mechanics these two mechanisms could be described in terms of stress intensity factors. For life time predictions the knowledge of subcritical crack growth and R- (respectively K_{R^-}) curve behavior of the material is essential.

The reduction of the material strength by temperature induced propagating microstructural cracks can be described as follows:

$$\sigma = \alpha \cdot \Delta T \frac{E_0}{1 + 2\pi N/l^2}$$

- σ effective strength
- α Coefficient of thermal expansion ($7 \dots 12 \cdot 10^{-6} \text{ 1/K}$)
- E_0 Modulus of elasticity
- N Number of temperature changes
- l Crack length

The brittleness of ferrite materials can be quantified by means of the fracture toughness. High fracture toughness values indicate decreased material brittleness. The quantity of the fracture toughness is a measure for the stress in the core necessary for a propagating crack. For the crack propagation it is required that the stress intensity factor exceeds the fracture toughness.

$$K_1 \geq K_{1C} \quad \text{with} \quad K_1 = \sigma_{\text{appl}} \sqrt{l \cdot Y} \quad \text{and} \quad K_{1C} = \sqrt{G_C E}$$

- K_1 Stress intensity factor
- K_{1C} Fracture toughness
- σ_{appl} applied stress
- Y Factor for fracture/sample geometry
- G_C Critical fracture area energy
- E Modulus of elasticity

Typical fracture toughness values can be obtained from the table on page 119.

Ferrite materials have a pronounced R-curve behavior, i. e. the fracture toughness increases with propagating crack length. In practice there is a rather tolerant behavior towards moderate single stress events.

8.2 Stress sensitivity of magnetic properties

Stresses in the core affect not only the mechanical but also the magnetic properties. It is apparent that the initial permeability is dependent on the stress state of the core. With

$$\mu_i \equiv \frac{1}{\frac{1}{\mu_{i0}} + k \cdot \sigma_T}; \quad k \approx 30 \cdot 10^{-6} \cdot \frac{1}{\text{MPa}}$$

General

Definitions

where μ_{i0} is the initial permeability of the unstressed material, it can be shown that the higher the stresses are in the core, the lower is the value for the initial permeability. Embedding the ferrite cores (e.g. in plastic) can induce these stresses. A permeability reduction of up to 50% and more can be observed, depending on the material. In this case, the embedding medium should have the greatest possible elasticity.

8.3 Magnetostriction

Linear magnetostriction is defined as the relative change in length of a magnetic core under the influence of a magnetic field. The greatest relative variation in length $\lambda = \Delta/l$ occurs at saturation magnetization. The values of the saturation magnetostriction (λ_s) of our ferrite materials are given in the following table (negative values denote contraction).

SIFERRIT material	K 12	K 1	N 48
λ_s in 10^{-6}	- 21	- 18	- 1,5

Magnetostrictive effects are of significance principally when a coil is operated in the frequency range < 20 kHz and then undesired audible frequency effects (distortion etc.) occur.

8.4 Resistance to radiation

SIFERRIT materials can be exposed to the following radiation without significant variation ($\Delta L/L \leq 1\%$ for ungapped cores):

gamma quanta:	10^9 rad
quick neutrons	$2 \cdot 10^{20}$ neutrons/m ²
thermal neutrons	$2 \cdot 10^{22}$ neutrons/m ²

8.5 Resistivity ρ , dielectric constant ϵ

At room temperature, ferrites have a resistivity in the range $1 \Omega\text{m}$ to $10^5 \Omega\text{m}$; this value is usually higher at the grain boundaries than in the grain interior. The temperature dependence of the core resistivity corresponds to that of a semiconductor:

$$\rho \sim e^{\frac{E_a}{k \cdot T}}$$

E_a Activation energy (0,1 ... 0,5 eV)

k Boltzmann constant

T Absolute temperature [K]

Thus the resistivity at 100°C is one order of magnitude less than at 25°C , which is significant, particularly in power applications, for the magnitude of the eddy-current losses.

Similarly, the resistivity decreases with increasing frequency.

Example: Material N 48

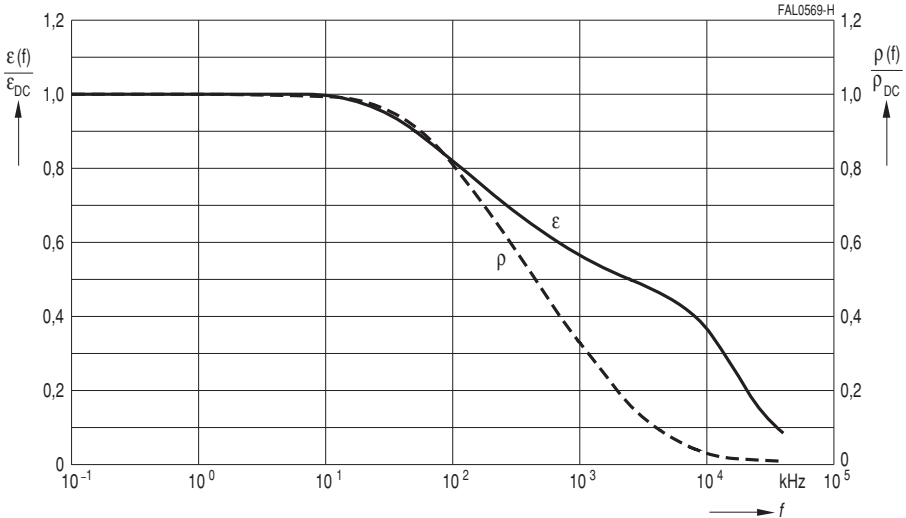


Fig. 8
Resistivity and dielectric constant versus frequency

The different resistivity values for grain interior and grain boundary result in high (apparent) dielectric constants ϵ at low frequencies. The dielectric constant ϵ for all ferrites falls to values around 10 ... 20 at very high frequencies. NiZn ferrites already reach this value range at frequencies around 100 kHz.

SIFFERIT material	Resistivity (approx.) Ωm	Dielectric constant ϵ at (approximate values)				
		10 kHz	100 kHz	1 MHz	100 MHz	300 MHz
K1 (NiZn)	10^5	30	15	12	11	11
N 48 (MnZn)	1	$140 \cdot 10^3$	$115 \cdot 10^3$	$80 \cdot 10^3$		

Magnetostrictive effects are of significance principally when a coil is operated in the frequency range < 20 kHz and then undesired audible frequency effects occur.

9 Coil characteristics
Resistance factor A_R

The resistance factor A_R , or A_R value, is the DC resistance R_{Cu} per unit turn, analogous to the A_L value.

$$A_R = \frac{R_{Cu}}{N^2}$$

When the A_R value and number of turns N are given, the DC resistance can be calculated from $R_{Cu} = A_R N^2$.

From the winding data etc. the A_R value can be calculated as follows:

$$A_R = \frac{\rho \cdot l_N}{f_{Cu} \cdot A_N}$$

where ρ = resistivity (for copper: 17,2 $\mu\Omega$ mm), l_N = average length of turn in mm, A_N = cross section of winding in mm^2 , f_{Cu} = copper space factor. If these units are used in the equation, the A_R value is obtained in $\mu\Omega = 10^{-6} \Omega$. For calculation of l_N and A_N the middle dimensions are used.

For coil formers, A_R values are given in addition to A_N and l_N . They are based on a copper filling factor of $f_{Cu} = 0,5$. This permits the A_R value to be calculated for any filling factor f_{Cu} :

$$A_{R(f_{Cu})} = A_{R(0,5)} \cdot \frac{0,5}{f_{Cu}}$$

For rough estimation a copper filling factor of $f_{Cu} = 0,5$ is sufficient. Else is given in the filling factor out of DIN 46435.

Herausgegeben von EPCOS AG

Marketing Kommunikation, Postfach 80 17 09, 81617 München, DEUTSCHLAND

© EPCOS AG 2000. Alle Rechte vorbehalten. Vervielfältigung, Veröffentlichung, Verbreitung und Verwertung dieser Broschüre und ihres Inhalts ohne ausdrückliche Genehmigung der EPCOS AG nicht gestattet.

Mit den Angaben in dieser Broschüre werden die Bauelemente spezifiziert, keine Eigenschaften zugesichert. Bestellungen unterliegen den vom ZVEI empfohlenen Allgemeinen Lieferbedingungen für Erzeugnisse und Leistungen der Elektroindustrie, soweit nichts anderes vereinbart wird.

Diese Broschüre ersetzt die vorige Ausgabe.

Fragen über Technik, Preise und Liefermöglichkeiten richten Sie bitte an den Ihnen nächstgelegenen Vertrieb der EPCOS AG oder an unsere Vertriebsgesellschaften im Ausland.

Bauelemente können aufgrund technischer Erfordernisse Gefahrstoffe enthalten. Auskünfte darüber bitten wir unter Angabe des betreffenden Typs ebenfalls über die zuständige Vertriebsgesellschaft einzuholen.

Published by EPCOS AG

Marketing Communications, P.O. Box 80 17 09, 81617 Munich, GERMANY

© EPCOS AG 2000. All Rights Reserved. Reproduction, publication and dissemination of this brochure and the information contained therein without EPCOS' prior express consent is prohibited.

The information contained in this brochure describes the type of component and shall not be considered as guaranteed characteristics. Purchase orders are subject to the General Conditions for the Supply of Products and Services of the Electrical and Electronics Industry recommended by the ZVEI (German Electrical and Electronic Manufacturers' Association), unless otherwise agreed.

This brochure replaces the previous edition.

For questions on technology, prices and delivery please contact the Sales Offices of EPCOS AG or the international Representatives.

Due to technical requirements components may contain dangerous substances. For information on the type in question please also contact one of our Sales Offices.